

Catalyst Promoted Synthesis, Computational and Enzyme Inhibition Studies of Coumarin Esters

Mehtab Parveen · Faheem Ahmad ·
Ali Mohammed Malla · Mahboob Alam ·
Dong-Ung Lee

Received: 23 August 2014 / Accepted: 28 September 2014 / Published online: 7 October 2014
© Springer Science+Business Media New York 2014

Abstract In the present study, a new series of ester analogues of substituted coumarin-3-carboxylic acids were synthesized which were typically accessed *via* a facile esterification reaction between propargyl alcohol and appropriately substituted coumarin-3-carboxylic acids (**1–5**). This new environmentally benign solid acid catalyst catalyzed, synthetic eco-friendly approach resulted in a noteworthy progress in synthetic efficiency (89–94 % yield), high purity, operational simplicity, mild reaction conditions, cleaner reaction profiles, recyclability of the catalyst and minimizing the production of chemical wastes without using highly toxic reagents for the synthesis. The molecular structure of compound **6** was authenticated by single crystal X-ray crystallographic analysis. The structure and morphology of the catalyst has been established on the basis of FT-IR, scanning electron microscopy–energy dispersion X-ray spectrometry and transmission electron microscopy. The promising bioactive score against enzymatic inhibition prompted us to carry out acetylcholinesterase inhibition screening of the synthesized compounds (**6–10**). A computer-aided molecular docking study was carried out to validate the specific binding mode of the newly synthesized compounds into the active site of

receptor to bear out the specific binding modes of the compounds.

Keywords Synthesis · Chromene-3-carboxylate · Catalyst · Silica-sulfuric acid · X-ray · AChE inhibition

1 Introduction

Over the years, coumarins have been established as the well-known naturally occurring oxygen containing heterocyclic compounds isolated from various plant sources as well as have been synthesized chemically [1]. They are structural subunits in many complex natural products and exhibit wide spectrum of pharmacological activities such as, antitumor [2], anti-HIV (NNRTI) [3], antioxidant [4], tumor necrosis factor- α (TNF- α) inhibition [5], antimicrobial [6], anti-inflammatory and antipyretic [7], antibacterial [8], antifungal [9], serine protease inhibition [10] and anticancer activities [11]. The studies have also shown that naturally occurring as well as the chemically synthesized coumarin analogs exhibit potent acetylcholinesterase (AChE) inhibitory activity [12]. Furthermore, functionalization of the coumarin nucleus has led to the development of novel analogs that are capable of inhibiting $A\beta$ aggregation [13]. The recognition of key structural features within coumarin template has helped in designing and synthesizing new analogs with improved AChE inhibitory activity and additional pharmacological activities including beta secretase (BACE) inhibition associated with decreased $A\beta$ deposition [14, 15] and monoamine oxidase (MAO) inhibition. Preliminary studies by employing *Torpedo californica* AChE revealed that coumarin and its derivatives are capable of interacting and inhibiting AChE by binding to PAS in a reversible manner [16, 17]. It led the

Electronic supplementary material The online version of this article (doi:10.1007/s10562-014-1381-7) contains supplementary material, which is available to authorized users.

M. Parveen (✉) · F. Ahmad · A. M. Malla
Department of Chemistry, Aligarh Muslim University,
Aligarh 202002, India
e-mail: mehtab.organic2009@gmail.com

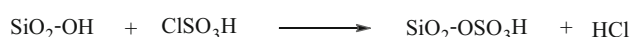
M. Alam · D.-U. Lee
Division of Bioscience, Dongguk University, Gyeongju 780-714,
Republic of Korea

scientists to make modifications in coumarin moiety to synthesize potent AChE inhibitors as potential candidates for managing Alzheimer's disease (AD) [18].

The synthesis of coumarin derivatives has previously been achieved by the use of various methods reported in the literature including the Pechmann [19], Perkin [20], Knoevenagel [21], Claisen [22], Reformatsky [23] and Wittig reactions [24]. In quest to achieve higher efficiency, several catalysts and reaction conditions were tried which include the use of microwave [25], nano-crystalline ZnO [26], heteropoly acids [27], tetrabutylammonium bromide [28], InCl_3 [29], molecular I_2 [30], PYBOX-DIPH-Zn(OTf) $_2$ complex [31], Cu(OTf)_2 [32], $\text{SiCl}_4/\text{EtOH}$ [33], bases such as K_2CO_3 [34], NaH [35], palladium-catalyzed base [36]. Earlier investigations required belated reaction times, use of costly and hazardous reagents and tedious workup procedures. In view of immense biological applications of coumarin derivatives, the development of simple and convenient protocol is of considerable interest.

In recent years, the use of silica supported catalysts [37–40] has received considerable attention due to growing environmental concerns. Such reagents not only simplify purification processes but also help in preventing the discharge of toxic reaction residues into the environment. In this respect silica supported sulfuric acid ($\text{SiO}_2\text{-OSO}_3\text{H}$) is an attractive candidate. It is a well known catalyst in organic synthesis and has been documented in several organic transformations [41–48]. Silica supported sulfuric acid ($\text{SiO}_2\text{-OSO}_3\text{H}$) catalyst was prepared by employing standard procedures depicted in the literature (Scheme 1) [49]. It possesses environmentally benign properties such as non-toxicity, biocompatibility, recyclability, physiological inertness, inexpensiveness, thermal stability. This new synthetic strategy resulted in a remarkable improvement in synthetic efficiency, minimizing the production of chemical wastes without using highly toxic reagent for the synthesis. In addition to efficacy, a major requirement of novel supported reagents concerns their reusability, a factor that has significant environmental and economic impact since the most costly components in a chemical reaction are often not the starting materials but the catalyst [50, 51]. The silica supported sulfuric acid is believed to be good proton source, which can give rise to lewis acid center on carbonyl carbon, followed by simultaneous attack of nucleophile to give corresponding coumarin derivatives.

Thus, based on the above findings and in continuation of our interest in the development of efficient, economical and



Scheme 1 Synthetic pathway for the synthesis of catalyst

new methodologies, we therefore, report a novel methodology for the synthesis of novel biologically active coumarin-3-carboxylic acid derivatives using silica supported sulfuric acid as the heterogeneous, environmentally benign solid acid catalyst. The efficacy of the catalyst was also examined. After a simple filtration, the catalyst was reused five times without a significant loss in yield. The structure and morphology of the catalyst was established on the basis of FT-IR, scanning electron microscopy–energy dispersion X-ray spectrometry (SEM–EDX) and transmission electron microscopy (TEM). The compounds were also screened for AChE inhibitory activity against standard drug tacrine. Moreover physicochemical calculations have been carried out in order to determine the relationship between the electronic properties and enzymatic inhibition activity of the synthesized compounds (6–10). The promising bioactive score of the synthesized compounds against enzymatic inhibition prompted us to carry out AChE inhibition screening of the synthesized compounds (6–10). A computer-aided molecular docking study was carried out to validate the specific binding mode of the newly synthesized compounds into the active site of receptor to bear out the specific binding modes of the compounds.

2 Experimental

2.1 Materials and General Methods

Chemicals were purchased from Merck and Sigma-Aldrich as 'synthesis grade' and used without further purification. Human recombinant AChE (EC: 3.1.1.7) lyophilized powder was purchased from Sigma-Aldrich. The IR spectra were recorded with Shimadzu IR-408 Perkin–Elmer 1800 (FTIR) and its values are given in cm^{-1} . ^1H NMR and ^{13}C NMR spectra were run in $\text{DMSO-}d_6$ on a Bruker Avance-II 400 MHz instrument with TMS as internal standard, J values are measured in Hertz. Chemical shifts are reported in ppm (δ) relative to the TMS. Mass spectra were recorded on a JEOL D-300 mass spectrometer. Melting points were determined on a Kofler apparatus and are uncorrected. Elemental analysis (%) C, H, N was conducted using Carlo Erba analyzer model 1108. Thin layer chromatography (TLC) glass plates (20×5 cm) were coated with silica gel G (Merck) and exposed to iodine vapors to check the homogeneity as well as progress of reaction.

2.2 Preparation of ($\text{SiO}_2\text{-OSO}_3\text{H}$) Catalyst

A 500 mL suction flask fitted with a constant pressure dropping funnel containing chlorosulphonic acid (23.3 g, 0.2 mol) and a gas inlet tube for conducting HCl gas over an absorbing solution (water). It was charged with silica gel

(60.0 g) and chlorosulphonic acid was added drop wise over a period of 30 min at room temperature, evolution of profuse amounts of HCl occurred instantaneously. After, the addition was completed the mixture was shaken well for 30 min, a white solid of silica-sulfuric acid (78.5 g) was obtained [49]. The various catalysts i.e. $\text{HClO}_4\text{-SiO}_2$ [52], $\text{NaHSO}_4\text{-SiO}_2$ [53], $\text{NH}_4\text{OAc-SiO}_2$ [54], $\text{P}_2\text{O}_5\text{-SiO}_2$ [55] and $\text{NH}_2\text{SO}_3\text{H-SiO}_2$ [56] used for the comparative study with respect to silica-sulfuric acid have been synthesized according to the previously published standard procedures.

2.3 Titration Analysis of ($\text{SiO}_2\text{-OSO}_3\text{H}$) Catalyst

The amount of H^+ in the silica-sulfuric acid catalyst was determined by acid–base titration according to the following reaction (Scheme 2). The liberated H_3O^+ was titrated by standard NaOH and the amount of H^+ in silica-sulfuric acid catalyst was calculated (0.05 g of silica sulfuric acid equal to 0.13 mmol).

2.4 General Method for the Synthesis of Prop-2-ynyl Derivatives of Substituted Coumarin-3-Carboxylic Acids

To a mixture of substituted coumarin-3-carboxylic acids (1–5) and propargyl alcohol (1 mmol) each, in dichloromethane (20 mL) was added silica supported sulfuric acid (2.5 mol %). The reaction mixture was allowed to stir at room temperature for 1.5–2 h. During stirring, the clear solution of reaction mixture began to turn thick and solid product precipitated. After completion of the reaction, as evident from TLC, the solid formed was filtered, washed with hot methanol to recover the catalyst. The filtrate containing soluble product was evaporated under reduced pressure to obtain crude product. The crude product obtained was washed with appropriate solvents, filtered, dried and crystallized from appropriate solvents. The catalyst was reused as such without a significant loss in yield.

2.4.1 Prop-2-yn-1-yl-2-oxo-2Hchromene-3-carboxylate, 6

Compound **6** recrystallized from $\text{CHCl}_3\text{-MeOH}$ as colorless crystals [57]; Yield: 93 %, mp 163 °C; Anal. Calc. for $\text{C}_{13}\text{H}_8\text{O}_4$; C, 68.42; H, 3.53; found: C, 68.44; H, 3.54. IR $\nu_{\text{max}}^{\text{KBr}}$ cm^{-1} : 2,118 ($\text{C}\equiv\text{C}$), 1,735 ($\text{C}=\text{O}$, ester), 1,713 ($\text{C}=\text{O}$, α -pyrone), 1,615, 1,563 ($\text{C}=\text{C}$). ^1H NMR (400 MHz, $\text{DMSO-}d_6$, δ , ppm): 8.81 (s, 1H, vinylic-H), 7.86–7.82 (m,



Scheme 2 Estimation of H^+ ion concentration in catalyst by acid base titration

1H, H-8), 7.75–7.72 (m, 1H, H-5), 7.44–7.40 (m, 2H, H-6, H-7), 4.93–4.94 (d, 2H, OCH_2), 3.31 (s, 1H, acetylenic proton). ^{13}C NMR (100 MHz, $\text{DMSO-}d_6$, δ , ppm): 163.5 ($\text{C}=\text{O}$, ester), 161.8 ($\text{C}=\text{O}$, α -pyrone), 154.7 (8a), 134.8 (CH), 130.5 (CH), 124.9 (CH), 117.8 (C-4), 116.7 (C-4a), 115.3 (C-3), 114.5 (CH), 78.2, 78.1 (acetylenic carbons), 52.8 (OCH_2). MS (ESI) m/z : 228 [$\text{M} + \text{H}$] $^+$.

2.4.2 Prop-2-yn-1-yl-7-hydroxy-2-oxo-2H-chromene-3-carboxylate, 7

Compound **7** recrystallized from $\text{CHCl}_3\text{-MeOH}$ as yellowish solid; Yield: 90 %, mp 245–246 °C; Anal. Calc. for $\text{C}_{13}\text{H}_8\text{O}_5$; C, 63.94; H, 3.30; found: C, 63.95; H, 3.34. IR $\nu_{\text{max}}^{\text{KBr}}$ cm^{-1} : 3,285 (OH), 2,123 ($\text{C}\equiv\text{C}$), 1,730 ($\text{C}=\text{O}$, ester), 1,710 ($\text{C}=\text{O}$, α -pyrone), 1,605, 1,561 ($\text{C}=\text{C}$). ^1H NMR (400 MHz, $\text{DMSO-}d_6$, δ , ppm): 8.79 (s, 1H, vinylic-H), 8.15 (s, 1H, OH), 7.89 (s, 1H, H-8), 7.52–7.48 (m, 1H, H-6), 7.45 (d, 1H, H-5), 4.63–4.64 (d, 2H, OCH_2), 3.12 (s, 1H, acetylenic proton). ^{13}C NMR (100 MHz, $\text{DMSO-}d_6$, δ , ppm): 162.3 ($\text{C}=\text{O}$, ester), 160.9 ($\text{C}=\text{O}$, α -pyrone), 157.2 (C–OH), 154.4 (8a), 140.8 (CH), 132.5 (CH), 128.6 (CH), 118.4 (C-4), 115.2 (C-4a), 114.7 (C-3), 76.2, 75.5 (acetylenic carbons), 51.4 (OCH_2). MS (ESI) m/z : 244 [$\text{M} + \text{H}$] $^+$.

2.4.3 Prop-2-yn-1-yl-7-methoxy-2-oxo-2H-chromene-3-carboxylate, 8

Compound **8** recrystallized from $\text{CHCl}_3\text{-MeOH}$ as colorless crystalline solid; Yield: 94 %, mp 176 °C; Anal. Calc. for $\text{C}_{14}\text{H}_{10}\text{O}_5$; C, 65.12; H, 3.90; found: C, 65.15; H, 3.92. IR $\nu_{\text{max}}^{\text{KBr}}$ cm^{-1} : 2,110 ($\text{C}\equiv\text{C}$), 1,725 ($\text{C}=\text{O}$, ester), 1,712 ($\text{C}=\text{O}$, α -pyrone), 1,615, 1,564 ($\text{C}=\text{C}$), 1,225 (C–O), ^1H NMR (400 MHz, $\text{DMSO-}d_6$, δ , ppm): 8.52 (s, 1H, vinylic-H), 7.78 (s, 1H, H-8), 7.55–7.51 (m, 2H, H-5, H-6), 4.71 (d, 2H, OCH_2), 3.85 (s, 3H, CH_3), 3.32 (s, 1H, acetylenic proton). ^{13}C NMR (100 MHz, $\text{DMSO-}d_6$, δ , ppm): 165.1 ($\text{C}=\text{O}$, ester), 160.2 ($\text{C}=\text{O}$, α -pyrone), 153.2 (C-7), 150.1 (8a), 130.4 (CH), 125.6 (CH), 122.3 (CH), 117.8 (C-4), 116.1 (C-4a), 113.4 (C-3), 78.4, 76.8 (acetylenic carbons), 56.1 (CH_3), 53.3 (OCH_2). MS (ESI) m/z : 258 [$\text{M} + \text{H}$] $^+$.

2.4.4 Prop-2-yn-1-yl-7-(diethylamino)-2-oxo-2H-chromene-3-carboxylate, 9

Compound **9** recrystallized from $\text{CHCl}_3\text{-MeOH}$ as yellowish solid; Yield: 91 %, mp 190 °C; Anal. Calc. for $\text{C}_{17}\text{H}_{17}\text{NO}_4$; C, 68.21; H, 5.72; N, 4.68; found: C, 68.22; H, 5.71; N, 4.67. IR $\nu_{\text{max}}^{\text{KBr}}$ cm^{-1} : 2,120 ($\text{C}\equiv\text{C}$), 1,720 ($\text{C}=\text{O}$, ester), 1,710 ($\text{C}=\text{O}$, α -pyrone), 1,606, 1,558 ($\text{C}=\text{C}$), 1,277 (C–N). ^1H NMR (400 MHz, $\text{DMSO-}d_6$, δ , ppm): 8.12

Table 1 Crystallographic data and structure refinement of compound (**6**)

Compound	6
Empirical formula	C ₁₃ H ₈ O ₄
Formula wt	228.19
Crystal system	Monoclinic
Space group	<i>P</i> 21/ <i>c</i>
<i>a</i> (Å)	6.7877 (10)
<i>b</i> (Å)	17.374 (2)
<i>c</i> (Å)	9.4835 (14)
α (°)	90
β (°)	110.642 (3)
γ (°)	90
<i>U</i> (Å ³)	1,046.6 (3)
<i>Z</i>	4
ρ_{calc} (Mg/m ³)	1.448
μ (mm ⁻¹)	0.109
<i>F</i> (000)	472
Refl. collected	6,504
Independent refl.	2,067
GOF	1.092
Final <i>R</i> indices	<i>R</i> ₁ = 0.0498 ^a
[<i>I</i> > 2 σ (<i>I</i>)]	<i>wR</i> ₂ = 0.1398 ^b
<i>R</i> indices (all data)	<i>R</i> ₁ = 0.0779 <i>wR</i> ₂ = 0.2166

$$^a R_1 = \frac{\sum \|F_o\| - |F_c|}{\sum \|F_o\|} \text{ with } F_o^2 > 2\sigma(F_o^2)$$

$$^b wR_2 = \left[\frac{\sum w(F_o^2 - |F_c^2|)^2}{\sum w F_o^4} \right]^{1/2}$$

(s, 1H, vinylic-H), 7.43 (s, 1H, H-8), 7.35–7.31 (m, 2H, H-5, H-6), 4.59 (d, 2H, OCH₂), 3.45 (q, 4H, N-CH₂), 3.20 (s, 1H, acetylenic proton), 1.21 (t, 6H, -CH₃). ¹³C NMR (100 MHz, DMSO-*d*₆, δ , ppm): 164.1 (C=O, ester), 162.4 (C=O, α -pyrone), 156.5 (C-8a), 149.3 (C-7), 127.4 (CH), 124.5 (CH), 123.0 (CH), 118.8 (C-4), 114.8 (C-4a), 113.4 (C-3), 78.7, 76.4 (acetylenic carbons), 52.5 (OCH₂), 45.4 (2 \times CH₂), 12.3 (2 \times CH₃). MS (ESI) *m/z*: 299 [M + H]⁺.

2.4.5 Prop-2-yn-1-yl-7-amino-2-oxo-2H-chromene-3-carboxylate, **10**

Compound **10** recrystallized from CHCl₃–MeOH as white solid; Yield: 89 %, mp 210 °C; Anal. Calc. for C₁₃H₉NO₄; C, 64.20; H, 3.73; N, 5.76; found: C, 64.22; H, 3.71; N, 5.77. IR $\nu_{\text{max}}^{\text{KBr}}$ cm⁻¹: 3,305 (NH₂), 2,130 (C \equiv C), 1,735 (C=O, ester), 1,715 (C=O, α -pyrone), 1,598, 1,553 (C=C), 1,267 (C–N). ¹H NMR (400 MHz, DMSO-*d*₆, δ , ppm): 8.09 (s, 1H, vinylic-H), 7.41 (s, 1H, H-8), 7.36–7.33 (m, 2H, H-5, H-6), 5.07 (s, 2H, NH₂, D₂O exchangeable), 4.55 (d, 2H, OCH₂), 3.17 (s, 1H, acetylenic proton). ¹³C NMR (100 MHz, DMSO-*d*₆, δ , ppm): 163.6 (C=O, ester), 161.7

(C=O, α -pyrone), 155.2 (C-8a), 147.2 (C-7), 129.3 (CH), 122.1 (CH), 121.4 (CH), 116.2 (C-4), 114.3 (C-4a), 110.2 (C-3), 77.4, 76.2 (acetylenic carbons), 50.4 (OCH₂). MS (ESI) *m/z*: 243 [M + H]⁺.

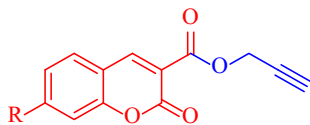
2.5 Single crystal X-ray Crystallographic Studies of Compound (**6**)

Single crystal X-ray data of compound **6** was collected at 100 K on a Bruker SMART APEX CCD diffractometer using graphite monochromated MoK α radiation (λ = 0.71073 Å). The linear absorption coefficients, scattering factors for the atoms and the anomalous dispersion corrections were taken from the International Tables for X-ray crystallography [58]. The data integration and reduction were carried out with SAINT software [59]. Empirical absorption correction was applied to the collected reflections with SADABS and the space group was determined using XPREP [60]. The structure was solved by the direct methods using SHELXTL-97 and refined on F² by full-matrix least-squares using the SHELXL-97 [61] program package. All non-hydrogen atoms were refined anisotropically. Pertinent crystallographic data for compound **6** is summarized in Table 1.

2.6 In Vitro Acetylcholinesterase Inhibition Activity

The ability of coumarin-3-carboxylic acid (COM-3) and synthesized compounds (**6**–**10**) to inhibit AChE activity was assessed by Ellman's method [62]. AChE stock solution was prepared by dissolving human recombinant AChE (EC: 3.1.1.7) lyophilized powder (Sigma-Aldrich) in 0.1 M phosphate buffer (pH 8.0) containing Triton X-100 (0.1 %). Five increasing concentrations of test compounds were assayed to obtain % inhibition of the enzymatic activity in the range of 20–80. The assay solution consisted of a 0.1 M phosphate buffer pH 8.0, with the addition of 340 μ M 5,5'-dithio-bis(2-nitrobenzoic acid), 0.02 unit/mL of human recombinant AChE from human serum and 550 μ M of substrate (acetylthiocholine iodide, ATCh). Increasing concentration of tested inhibitor were added to the assay solution and pre-incubated for 5 min at 37 °C with the enzyme followed by the addition of substrate. Initial rate assays were performed at 37 °C with a Jasco V-530 double beam Spectrophotometer. Absorbance value at 412 nm was recorded for 5 min and enzyme activity was calculated from the slope of the obtained linear trend. Assays were carried out with a blank containing all components except AChE to account for the non-enzymatic reaction. The reaction rates were compared and the percent inhibition due to the presence of tested inhibitors was calculated. Each concentration was analyzed in triplicate, and IC₅₀ values were determined graphically from log concentration–inhibition curves (GraphPad Prism 4.03

Table 2 Quantitative estimation of acetylcholinesterase inhibition activity of compounds (**6–10**) by modified Ellaman's coupled enzyme assay method using tacrine as reference



S. No.	Product	Nature of substituents (R)	IC ₅₀ (μM) ^a ± SEM for hAChE inhibition
1	COM-3	–	0.59 ± 0.01
2	6	R=H	0.35 ± 0.01
3	7	R=OH	0.24 ± 0.01
4	8	R=OCH ₃	0.33 ± 0.01
5	9	R=N(CH ₃ CH ₂) ₂	0.54 ± 0.01
6	10	R=NH ₂	0.21 ± 0.01
7	(Tacrine) standard		0.19 ± 0.01

COM-3 coumarin-3-carboxylic acid (**1**), SEM standard error of the mean, hAChE human recombinant AChE

^a IC₅₀ = Concentration of inhibitor required to decrease enzyme activity by 50 %

software, GraphPad Software Inc.). Tacrine was used as a standard inhibitor. AChE inhibition activity of synthesized compounds is presented in Table 2.

2.7 Computational Methods

Molinspiration online database was used to calculate fourteen descriptors (www.molinspiration.com), which are logP, polar surface area, molecular weight, number of hydrogen bond donor, number of hydrogen bond acceptor, number of violation to Lipinski's rule, number of rotatable bonds, volume, drug likeness includes G protein coupled receptor (GPCR) ligand, ion channel ligand, kinase inhibitor, nuclear receptor ligand, protease inhibitor and enzyme inhibitor, for all synthesized ligands. The method for calculation of MologP was developed by Molinspiration (miLogP 2.2—2005) programme, based on group contributions. Group contributions have been obtained by fitting calculated logP with experimental logP for a training set of more than twelve thousand of drug-like molecules. Molecular polar surface area (TPSA) was calculated relied based on the published methodology [63], which is virtually a sum of fragment-based contributions. The maps of molecular lipophilicity potential (MLP) and polar surface area (TPSA) were viewed in Molinspiration Galaxy 3D Structure Generator.

2.8 Molecular Docking

The retrieved protein (PDB: 4ey4) used for this purpose was improved by using import and preparation option of MVD software [64] and missing bond order, hybridization

state, angle and flexibility for achieving reliable potential binding site in the receptor. All the compounds were designed and structures were analyzed using Chem Draw Ultra3D software and then these structures were energetically minimized using MM2 force field with RMS gradient set to 0.0001 and coordinates of compounds were checked using PRODRG programme [65]. Hex6.1 [66], Discovery studio 4.0 Client [67] and iGEMDOCK [68] softwares were used to sort out top ten molecular docking poses of ligand (compound)–receptor interactions, perform visualization of docked ligands and illustration of basic features of the docked interface and compute energy calculation of docked ligands, respectively.

3 Results and Discussions

3.1 Characterization of the Silica-Sulfuric Acid Catalyst

The FT-IR spectrum of the catalyst is shown in Fig. 1. The IR spectrum was recorded using the KBr disk technique. For silica (SiO₂), the major peaks are broad anti symmetric Si–O–Si stretching from 1,200 to 1,000 cm⁻¹ and symmetric Si–O–Si stretching near 800 cm⁻¹. For sulfuric acid functional group, the FT-IR absorption range of the O=S=O asymmetric and symmetric stretching modes lies in 1,120–1,230 and 1,010–1,080 cm⁻¹ respectively, and that of the S–O stretching mode lies in 600–700 cm⁻¹. FT-IR spectrum displays the overlap asymmetric and symmetric stretching bands of SO₂ with Si–O–Si stretching bands in the silica sulfuric acid. The spectrum also shows a broad OH stretching absorption around 3,440 cm⁻¹.

To study the surface morphology of the catalyst, SEM analysis of the catalyst was employed. An examination of SEM images (Fig. 2) showed that catalyst particles were of uneven shape and size, well distributed and no conglomeration of catalyst particles was found on the surface of the silica gel. The increased reactivity of sulfuric acid supported on silica material could be possibly due to the catalyst–support interactions and the resultant changes in the surface properties of the reactive sites. TEM image (Fig. 3) further showed uniform distribution of catalyst particles as black dots on the surface of silica, confirming the formation of the expected catalytic system. EDX analysis (Fig. 4) of the catalyst showed the presence of Si, S and O elements suggesting the formation of SiO₂–OSO₃H catalytic system.

3.2 Chemistry

The synthetic pathway of a series of new ester derivatives of coumarin-3-carboxylic acid (**6–10**) is shown in

Fig. 1 FT-IR spectrum of catalyst $\text{SiO}_2\text{-OSO}_3\text{H}$

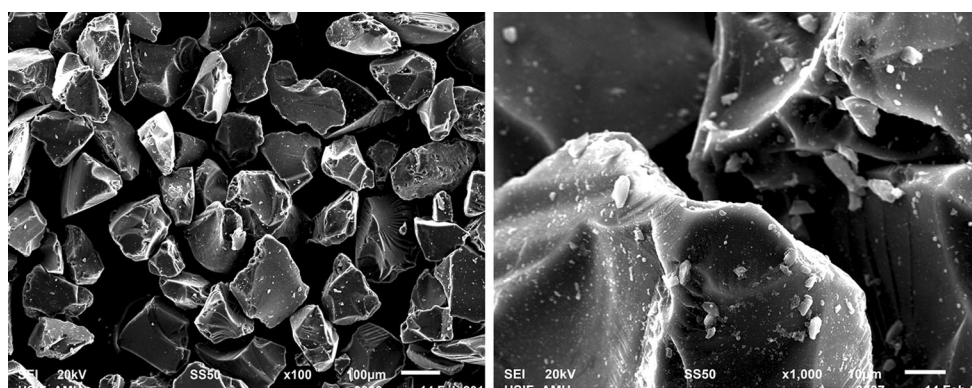
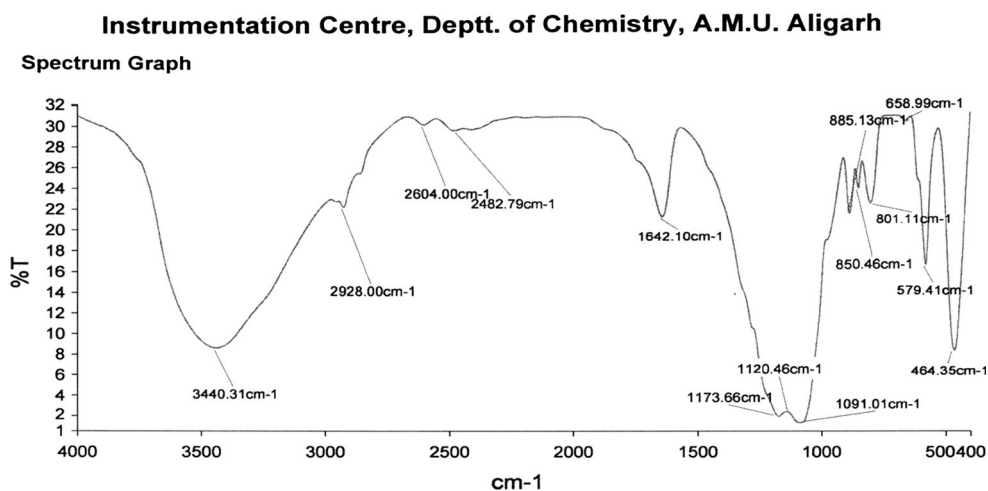


Fig. 2 SEM image of catalyst $\text{SiO}_2\text{-OSO}_3\text{H}$

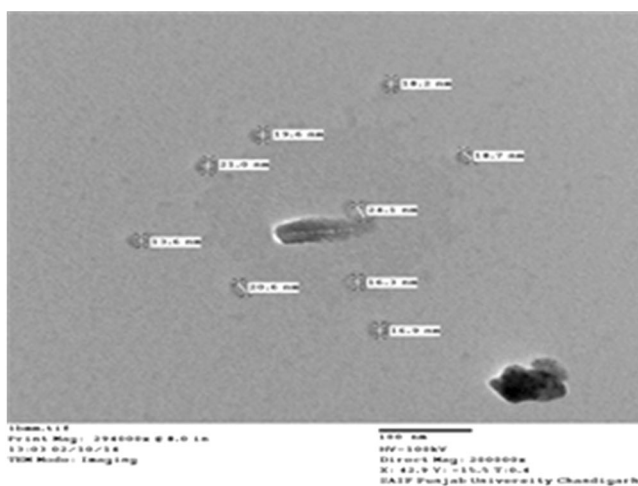
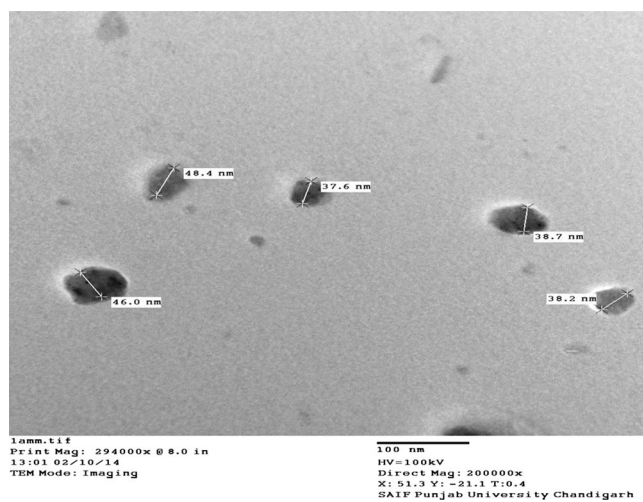


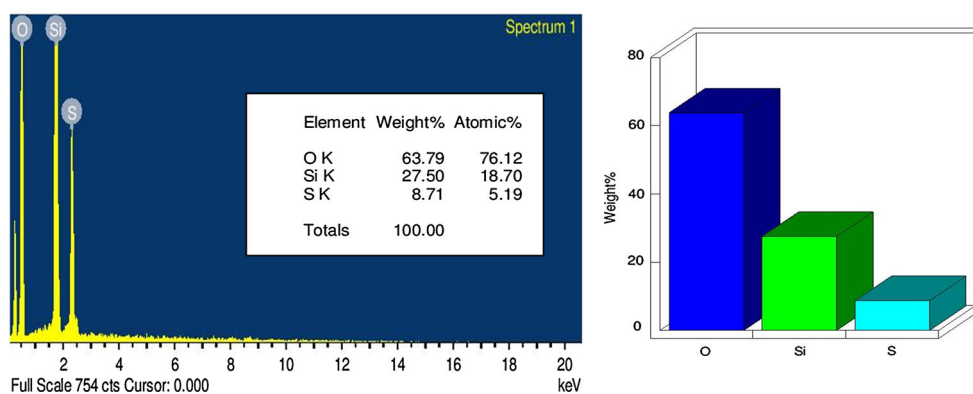
Fig. 3 TEM image of catalyst $\text{SiO}_2\text{-OSO}_3\text{H}$

Scheme 3. Herein series of compounds were typically accessed *via* a facile esterification reaction of substituted coumarin-3-carboxylic acids (**1–5**) and propargyl alcohol. All the compounds were obtained in excellent yields (89–94 %) with high purity. The molecular structure of

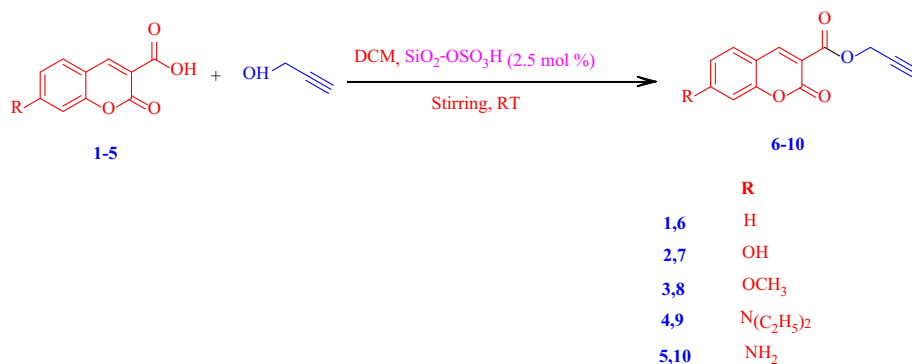
compound (**6**) was further supported by single crystal X-ray crystallographic analysis.

The structural elucidation of the synthesized compounds (**6–10**) was established on the basis of elemental analysis, IR, ^1H NMR, ^{13}C NMR and Mass spectral studies. The

Fig. 4 Energy dispersive X-ray (EDX) analysis of catalyst $\text{SiO}_2\text{-OSO}_3\text{H}$



Scheme 3 Synthetic pathway for the synthesis of ester derivatives of substituted coumarin-3-carboxylic acids (**6–10**)



analytical results for C, H, N, were within $\pm 0.3\%$ of the theoretical values. All the synthesized compounds displayed characteristic peaks for α -pyrone carbonyl of coumarin nucleus, ester carbonyl and acetylenic group, resonating at around 1,710–1,715, 1,720–1,735 and 2,110–2,130 cm^{-1} respectively. Moreover absorption bands resonating at 3,285 and 3,305 cm^{-1} in compounds **7** and **10**, are ascribed to OH and NH_2 groups respectively.

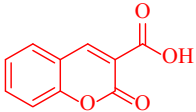
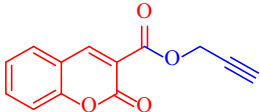
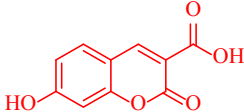
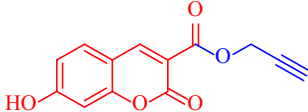
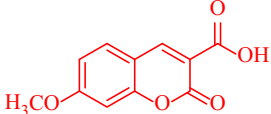
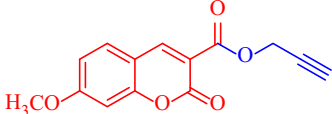
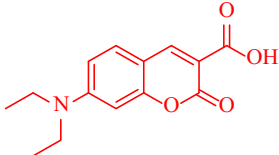
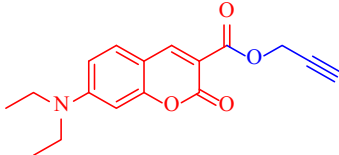
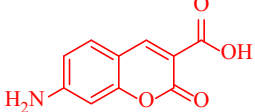
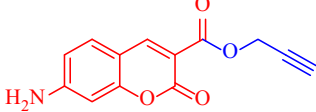
In ^1H NMR, each compound displayed a sharp singlet around δ 8.09–8.81, attributed to vinylic proton (H-4) of coumarin nucleus, this prominent downfield shift displayed by H-4 protons is attributed to their hydrogen bonding with adjacent ester carbonyl oxygen. A sharp singlet and a doublet peak, integrating for one and two protons each, resonating at δ 3.12–3.31 and 4.55–4.94 is ascribed to acetylenic ($\equiv\text{C-H}$) and methyleneoxy ($-\text{OCH}_2$) protons respectively. Similarly peaks for aromatic protons are already discussed in experimental section. In ^{13}C NMR, characteristic absorption bands resonating at around δ 160.2–160.4, 162.3–165.1, 50.4–53.3 and 75.5–78.7 were ascribed to carbonyl moiety of coumarin nucleus, ester carbonyl, methyleneoxy carbon ($-\text{OCH}_2$) and acetylenic carbons ($-\text{C}\equiv\text{CH}$), respectively. A sharp absorption signal at δ_{C} 157.2 in case of compound **7** is ascribed to hydroxylated (C-7) carbon. Besides, a series of signals emerging at around δ 121.4–140.8 is ascribed to aromatic carbons.

Mass spectral analysis was also in agreement with the proposed structure of the compounds.

In order to develop eco-friendly approach, we explored efficacy of silica supported sulfuric acid ($\text{SiO}_2\text{-OSO}_3\text{H}$) by carrying out the reaction of propargyl alcohol with a variety of substituted coumarin-3-carboxylic acids in equimolar ratio (1:1), at room temperature. The reaction proceeded smoothly and resulted in the formation of corresponding products (**6–10**) in excellent yields (89–94 %) within (1.5–2 h) as monitored by TLC (Table 3). The plausible reaction mechanism for the synthesis of target compounds (**6–10**) is shown in Scheme 4.

In order to optimize the reaction conditions a model reaction was conducted using coumarin-3-carboxylic acid (**1**, 1 mmol) and propargyl alcohol (1 mmol) under various reaction conditions (including loading of catalyst, effect of solvents in terms of yields and time). In order to establish the best reaction conditions, we performed an optimization study using model substrate in the presence of varying amounts of catalyst ($\text{SiO}_2\text{-OSO}_3\text{H}$) (Table 4). The model reaction was primarily, tested in absence of catalyst, it was found that reaction took prolonged time for completion with meager yield. It can be inferred from (Table 4, entry 6) that 2.5 mol% of the catalyst is sufficient to get optimum yield in shorter reaction time. Using less than 2.5 mol% catalyst (0.5, 1, 1.5, 2 mol%) moderate yield of the product

Table 3 Silica supported sulfuric acid (SiO₂-OSO₃H) catalyzed synthesis of coumarin-3-carboxylic acid derivatives (6–10)

S. No.	Reactants	Products	Time ^a (h)	Yield ^b (%)	MP (°C)
1			2	93	163
2			1.5	90	245–246
3			1.5	94	176
4			2	91	190
5			2	89	210

^a Reaction progress monitored by TLC

^b Isolated yield of products

(65–85 %) was obtained with higher reaction time, while with excess mol% of catalyst (>2.5 mol%) there was no further increment in the yield of the product probably due to the saturation of the catalyst surface. In order to study the solvent effect, the model reaction was carried out in different solvent systems. The reaction was initially, tested under solvent-free condition by grinding method, however only traces of product were obtained (Table 5, entry 1). When the reaction was performed in CH₃OH and CH₃CH₂OH, moderate yield of the products were obtained after prolonged time period (Table 5, entry 5, 6). This can be attributed to the nucleophilic nature of these solvents, due to presence of lone pair of electrons on oxygen atom. Thus nucleophilic competition between these solvents (MeOH, EtOH) and propargyl alcohol for electrophilic carbonyl carbon of acid will eventually resulted in low yield of desired product. Whereas in acetic acid, reaction again took longer time period (Table 5, entry 4) but there was an improvement in yield, probably CH₃COOH facilitates the formation of carbocation by activating the carbonyl group of coumarin acid, thus enhances the electrophilicity of carbonyl carbon, rendering it more feasible for nucleophilic attack. However there was noteworthy improvement in the yield when tetrahydrofuran

(THF) was used as a solvent (Table 5, entry 3). When the reaction was carried out in CH₂Cl₂ (Table 5, entry 2), the yield of the product improved significantly in shorter time period. A comparative study of variety of silica supported catalysts was conducted to confirm the superiority of silica-sulfuric acid as a heterogeneous acid catalyst. The model reaction was initially conducted in absence of catalyst, the reaction took prolonged time and yield was less than 50 % (Table 6, entry 1). When the model reaction was investigated with heterogeneous catalysts such as NaHSO₄-SiO₂, NH₄OAc-SiO₂, P₂O₅-SiO₂ and NH₂SO₃H-SiO₂, the reaction took extended time period, and yields were not satisfactory (Table 6, entry 4–7). It was found that, the yield of the product increased significantly when HClO₄-SiO₂ was added to the model reaction, probably due to its facile proton release which catalyzes the reaction (Table 6, entry 3). However there was noteworthy improvement in the yield and reduction in reaction time when HO₃SO-SiO₂ was employed as a catalyst (Table 6, entry 2).

The reusability of the silica-chloride catalyst was also examined on model reaction. The catalyst was reused five times and the results demonstrate that catalyst can be reused as such without a significant loss in yield (Table 7). After the first fresh run with 93 % yield, the catalyst was

Scheme 4 Plausible mechanistic catalytic loop for the synthesis of compounds (6–10)

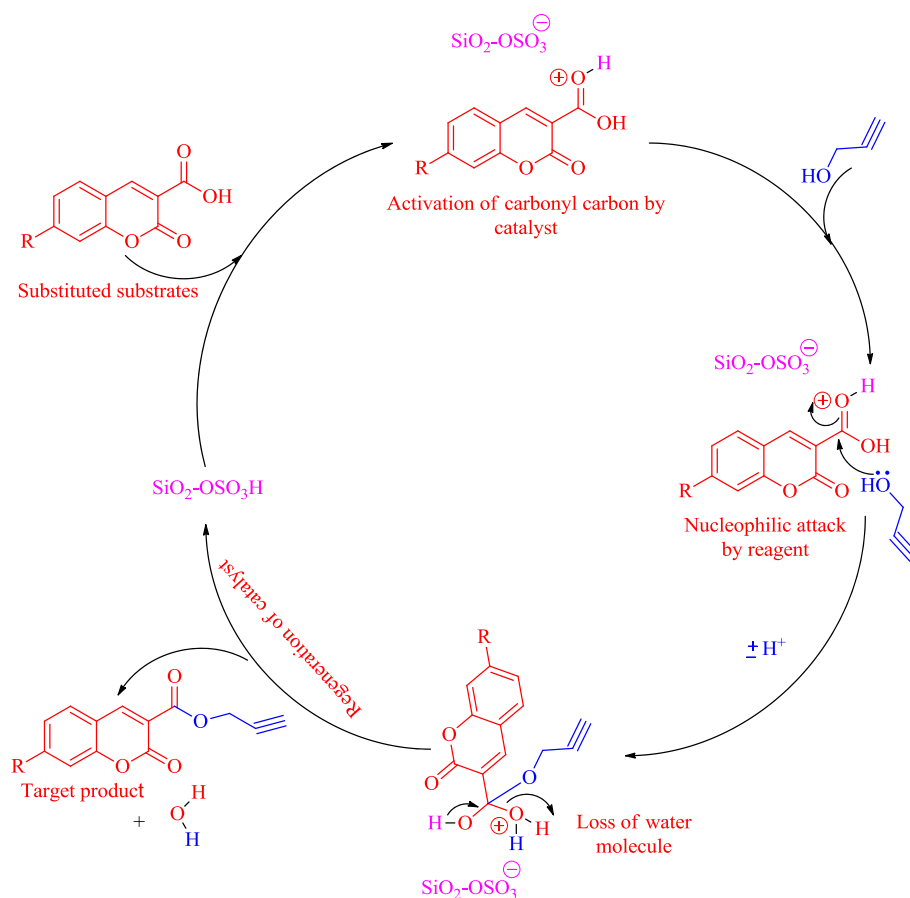


Table 4 Effect of catalyst loading on the synthesis of compound (6)

Entry	Catalyst (mol%)	Time (h) ^a	Yield (%) ^b
1	No catalyst	9	57
2	0.5	7	65
3	1.0	6	73
4	1.5	4	81
5	2.0	3	85
6	2.5	2	93
7	3.0	2	93

Reaction condition: coumarin-3-carboxylic acid (**1**, 1 mmol), propargyl alcohol (1 mmol), stirring, room temperature (25 °C), solvent DCM

^a Reaction progress monitored by TLC

^b Isolated yield of products

removed by filtration. The recovered catalyst was dried under vacuum at 120 °C for 10 h and tested up to five more reaction cycles. Recycling and reuse of the catalyst showed minimal decreases in yields. The product **6** was obtained in 90, 88, 85, 81, 81 % yields after successive cycles. (Table 7, entries 2–6), thus proving the catalyst's reusability. To ascertain the variation in morphological features

Table 5 Effect of various solvents on model reaction

Entry	Solvent	Time (h) ^a	Yield (%) ^b
1	Solvent free ^c	–	Traces
2	CH_2Cl_2	2	93
3	THF	5.5	73
4	CH_3COOH	7	67
5	CH_3OH	9	63
6	$\text{CH}_3\text{CH}_2\text{OH}$	>10	54

Reaction condition: Coumarin-3-carboxylic acid (**1**, 1 mmol), propargyl alcohol (1 mmol), catalyst (2.5 mol %), different solvents (20 mL), stirring at RT

^a Reaction progress monitored by TLC

^b Isolated yield of products

^c Solvent free by grinding method

of the recovered catalyst, we carry out its SEM–EDX analysis. It was observed that the composition of the catalytic system was almost consistent with the fresh catalyst (Fig. S1, see supplementary information) and also there was no significant change in the morphology of the catalyst (Fig. 5) as compared to the fresh catalyst.

Table 6 Comparison of catalytic activity of different silica supported catalysts on themodel reaction (**6**)

Entry	Catalyst	Time (h) ^a	Yield (%) ^b
1	–	>13	47
2	HO ₃ SO–SiO ₂	2	93
3	HClO ₄ –SiO ₂	5	70
4	NaHSO ₄ –SiO ₂	7	63
5	NH ₄ OAc–SiO ₂	6	67
6	P ₂ O ₅ –SiO ₂	8.5	59
7	NH ₂ SO ₃ H–SiO ₂	8	55 (Impure)

Reaction condition: coumarin-3-carboxylic acid (**1**, 1 mmol), propargyl alcohol (1 mmol), stirring, room temperature (25 °C), different catalysts (2.5 mol %), solvent DCM

^a Reaction progress monitored by TLC

^b Isolated yield of products

Table 7 Reusability of (SiO₂-OSO₃H) catalyst in the synthesis of compound (**6**)

Entry	Reaction cycle	Isolated yield (%) ^a
1	1st (Fresh run)	93
2	2nd cycle	90
3	3rd cycle	88
4	4th cycle	85
5	5th cycle	81
6	6th cycle	81

Reaction condition: coumarin-3-carboxylic acid (**1**, 1 mmol), propargyl alcohol (1 mmol), stirring, room temperature (25 °C), catalyst (2.5 mol %), solvent DCM

^a Isolated yield of products

3.3 X-ray Crystallographic Study

Compound **6**, once isolated, was found to be air-stable and soluble in all common organic solvents but insoluble in water. X-ray crystallographic analysis reveals that compound **6**

crystallizes in the monoclinic structure with space group P21/c. The asymmetric unit of compound **6** is shown in Fig. 6, while other crystallographic parameters are listed in Table S1, S2, S3, S4 and S5 (see supplementary information).

3.4 AChE Inhibition Results

The parent coumarin-3-carboxylic acid (COM-3) and all the synthesized compounds (**6–10**) substituted with different groups were analyzed for AChE inhibition activity. It can be inferred from the data shown in Table 2, that compound **10**, exhibited the strongest inhibition to AChE with an IC₅₀-value of 0.21 μM, followed by compound **7** (IC₅₀ = 0.24 μM), **8** (IC₅₀ = 0.33 μM), **6** (IC₅₀ = 0.35 μM) and **9** (IC₅₀ = 0.54 μM). The results indicate that all the tested compounds displayed significant AChE inhibitory activity except compound **9**. On close examination of the data reported in Table 2, it can be observed that the substituent at C-7 position of the coumarin nucleus inflict prominent effect on the AChE inhibition. When the hydrogen atom at C-7 position in compound **6** (IC₅₀ = 0.35 μM) is replaced by OH group (compound **7**), there was significant increase in the AChE inhibitory activity by ±0.11 value. The replacement of hydrogen atom in compound **6** at C-7 by methoxy (OCH₃) group (compound **8**) leads to a slight increase in the activity by ± 0.02 value. However when the same hydrogen atom was replaced by diethyl amine N(CH₃CH₂)₂ group (compound **9**), there was prominent decrease in AChE activity by ±0.19 value. This significant dip in activity of compound **9** is probably due to the bulky substituent N(CH₃CH₂)₂ at C-7 position of coumarin nucleus which restricts it to fit better inside the cavity of AChE. It was observed that the substitution of hydrogen atom in compound **6** by amine (NH₂) group (compound **10**), exceptionally enhanced the AChE activity by ±0.14 value with IC₅₀ value of 0.21 μM almost comparable to standard drug tacrine (IC₅₀ = 0.19 μM).

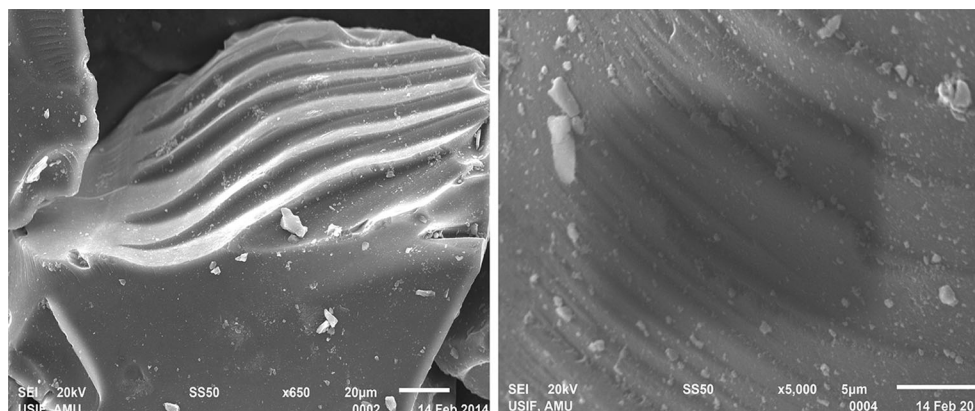
**Fig. 5** SEM image of recovered catalyst after five runs at different magnifications

Fig. 6 Asymmetric unit showing (a) thermal ellipsoid (50 %) plot and (b) ball and stick model of compound (6)

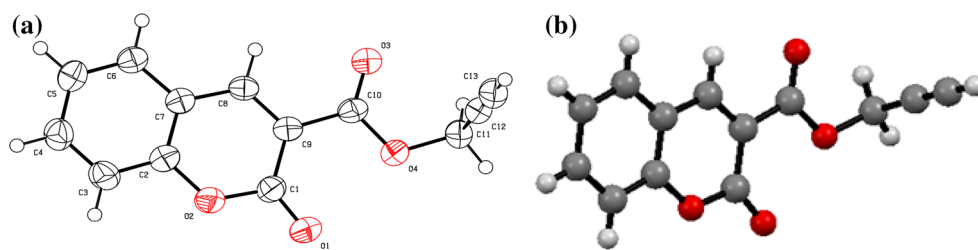
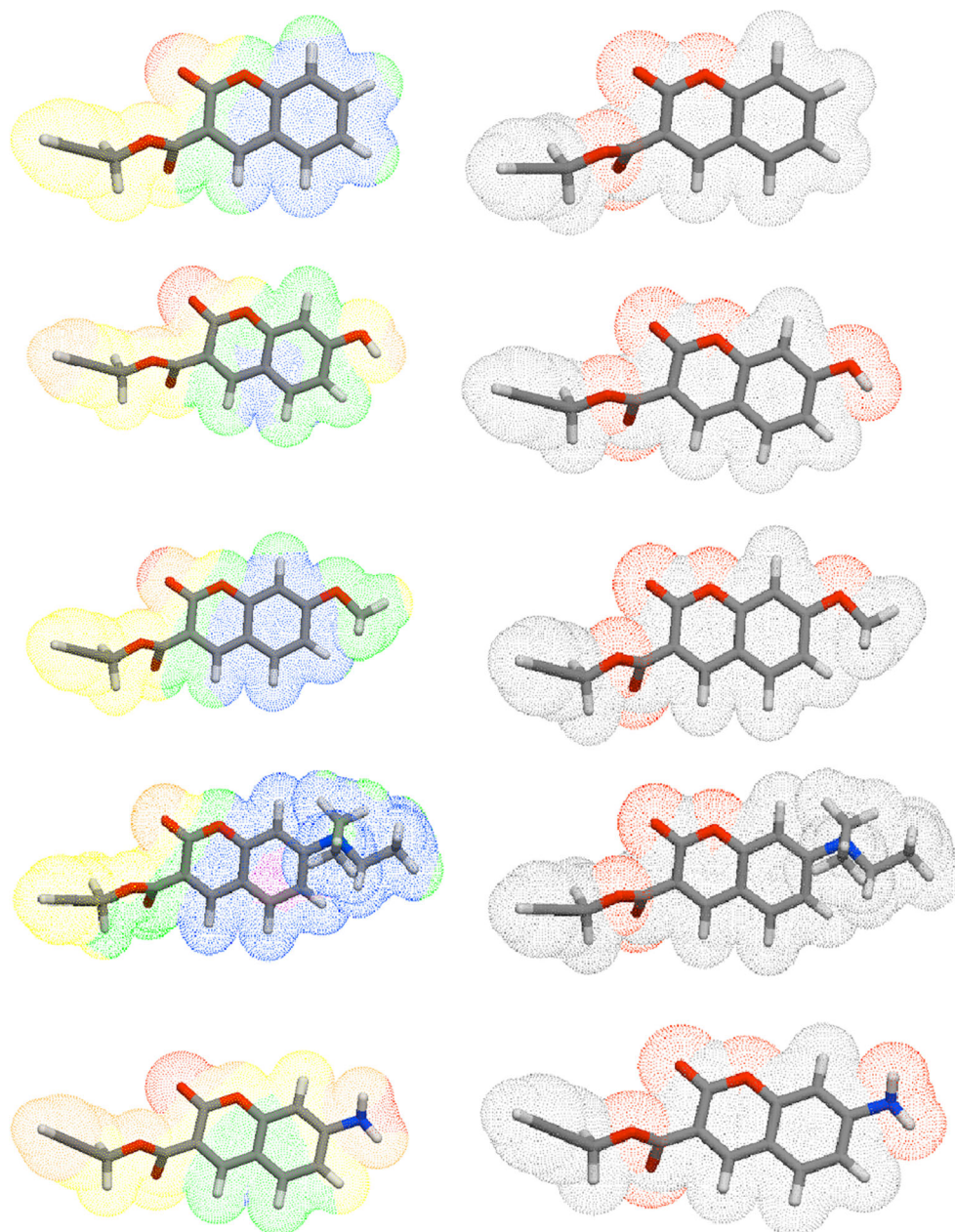


Fig. 7 3D sketch of the compounds (6–10) with molecular lipophilicity (left side) and polar surface pockets (right side) showing the most lipophilic area (pink color), intermediate lipophilic area (green color), most hydrophobic area (blue color), nonpolar area (gray white color) and polar area (red color) (Color figure online)



In order to study the effect of appended propargyl group in coumarin esters (6–10) on the AChE activity, we have also analyzed parent coumarin-3-carboxylic acid (1) for

AChE inhibition. It can be inferred from the data reported in the Table 2, that there has been prominent increase in AChE inhibition of compound 6 by appending propargyl

Table 8 Drug likeness score of synthesized compounds (6–10)

Compound	MW (g/mol)	miLogP ^a	TPSA ^b	nOHNH ^c	nON ^d	Nrotb ^e	n violation	Volume
COM-3	190.154	1.514	67.51	1	4	1	0	155.588
6	228.203	1.934	56.516	0	4	3	0	195.615
7	224.202	1.43	76.744	1	5	3	0	203.633
8	258.229	1.966	65.75	0	5	4	0	221.161
9	299.326	2.764	59.754	0	5	6	0	275.124
10	243.218	0.986	82.539	2	5	3	0	206.904
(Tacrine) standard	198.269	3.05	38.915	2	2	0	0	191.533

COM-3 Coumarin-3-carboxylic acid (**1**)

^a Calculated octanol/water partition coefficient

^b Molecular polar surface area

^c Number of hydrogen-bond donors

^d Number of hydrogen-bond acceptors

^e Number of rotatable bonds

Table 9 Bioactivity score of the synthesized compounds (6–10)

Compounds	GPCR ligand	Ion channel ligand	Kinase inhibitor	Nuclear receptor ligand	Protease inhibitor	Enzyme inhibitor
COM-3	−1.03	−0.84	−1.21	−0.42	−0.76	−0.18
6	−0.73	−0.67	−0.94	−0.24	−0.64	−0.11
7	−0.61	−0.61	−0.78	0.05	−0.57	0.00
8	−0.64	−0.73	−0.79	−0.10	−0.58	−0.11
9	−0.39	−0.57	−0.58	0.10	−0.37	−0.12
10	−0.62	−0.56	−0.74	−0.24	−0.47	0.02
(Tacrine) standard	−0.11	0.36	−0.37	−0.93	−0.59	0.43

COM-3 coumarin-3-carboxylic acid (**1**)

Active = Score more than 0.00; Moderately active = Score between −0.50 and 0.00; Inactive = Score less than −0.50

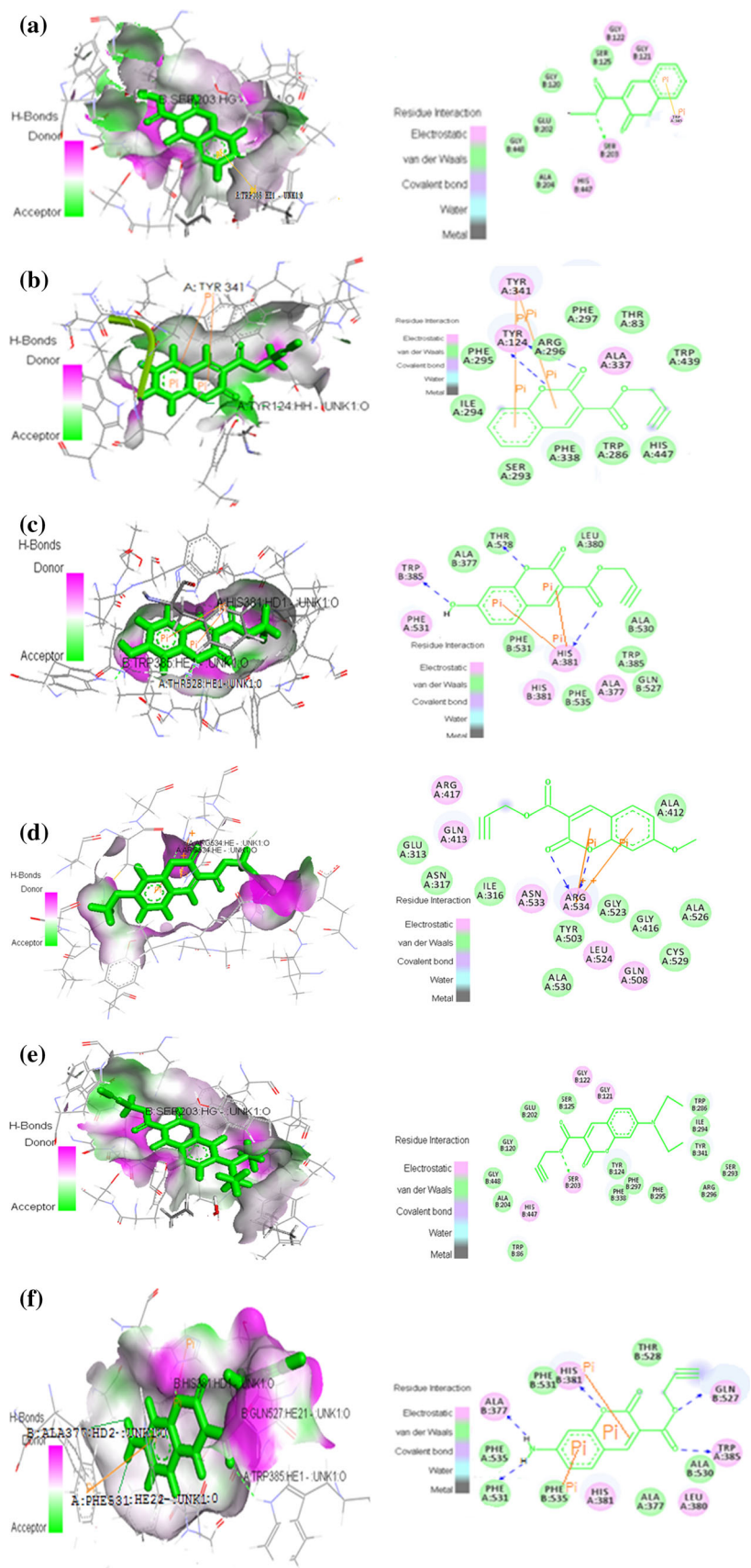
group to the parent coumarin-3-carboxylic acid (**1**) by ± 0.24 value. This suggests that incorporation of propargyl group inflict a noticeable effect on AChE inhibition. The enzyme inhibition activity of parent coumarin acid (**1**) ($IC_{50} = 0.59 \mu M$) was found to be less in comparison to all the synthesized compounds (**6–10**). It was found that the nature of substituent and appended propargyl group in the synthesized coumarin esters (**6–10**) are believed to inflict effect on AChE activity. The results obtained were well supported by the docking studies in which parent coumarin acid (**1**) displayed poor interaction with the target protein (PDB: 4ey4).

3.5 Molecular Properties Prediction and Drug-Likeness Results

The prediction of absorption, distribution, metabolism and excretion (ADME) properties of the parent coumarin acid (**1**) and synthesized compounds (**6–10**) were calculated to depict molecular properties essential for a drug pharmacokinetics in the human body. The physicochemical

parameter such as Polar surface area (TPSA), MilogP, number of hydrogen bond donor and acceptor atoms, number of rotatable bonds, molecular volume and violations of Lipinski's rule of five were premeditated using Molinspiration online property calculation toolkit. Basically, Molinspiration is a cheminformatic software tool which computes the molecular properties of any chemical structure as well as bioactivity score for the most important drug targets such as GPCR ligands, ion channel ligand, kinase inhibitors, nuclear receptor ligand, protease inhibitor and enzyme inhibitor. Membrane permeability and bioavailability are associated with some basic molecular descriptors such as partition coefficient (MiLogP), molecular weight (MW), hydrogen bond acceptors (HBA) and hydrogen bond donors (HBD) count in a molecule. Moreover, number of rotatable bonds is also important to predict the conformational changes and flexibility for binding with receptor or channels. The TPSA is a signifier for the anticipation of passive molecular transport through membranes. The combined parameters, TPSA and molecular volume are inversely proportional to percentage absorption

Fig. 8 Available binding sites for parent coumarin acid (**1**) and compounds (**6–10**; UNK) and target enzyme (PDB: 4ey4) displaying various interactions with amino acids residues at active site of target protein (**a** = 3D active Site and **b** = 2D ligand–receptor interaction diagrams)



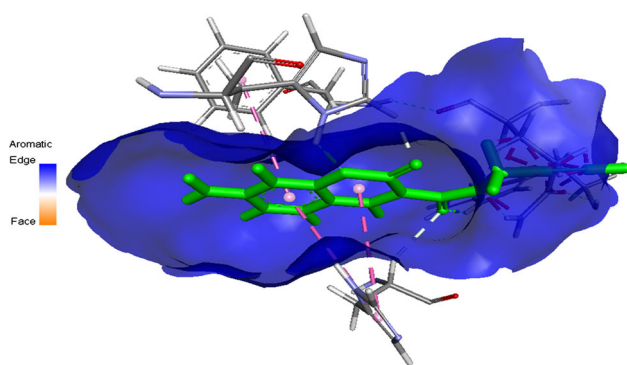
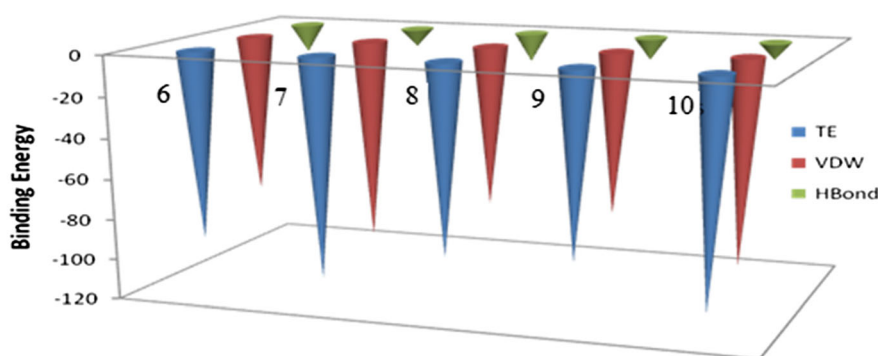


Fig. 9 π - π interaction of compound **10** with amino acid residues PHE535 and HIS381 of target enzyme

(% ABS) and predict the nature of transport properties of drugs in the intestines and blood-brain barrier crossing. All the compounds (**6–10**) showed zero violations of Lipinski's "Rule of Five" which indicated their presence for bioavailability. The molecular lipophilicity potential (MLP) map and polar surface areas (TPSAs) of compounds are shown in Fig. 7 and Table 8. On the close inspection of Table 8, all the synthesized compounds were found in good agreement with Lipinski's rules for new chemical entity to have good oral bioavailability with no violations. The MologP values of all the compounds was found within the range of 0.986–2.764 (<5), without exception, suggesting that these will be soluble in aqueous solution and hence will be able to gain access to membrane surfaces. Moreover the values of TPSA are within the limit i.e. 82 Å, indicating a good permeability of the drug in the cellular plasma membrane. The upper limit for TPSA for a molecule to penetrate the brain is around 90 Å.

The bioactivity score was also calculated for GPCR ligand, ion channel ligand, kinase inhibitor, nuclear receptor

Fig. 10 Estimated binding affinities of synthesized compounds (**6–10**) based on docked poses within active site of target enzyme (PDB: 4ey4)



	6	7	8	9	10
TE	-93.1646	-108.594	-93.1646	-90.7099	-110.146
VDW	-78.7424	-99.5293	-78.7424	-79.561	-101.483
HBond	-14.4222	-9.06511	-14.4222	-11.1489	-8.66262

TE = Total energy
VDW = Vander waals energy
HBond = Hydrogen bonding energy

ligand, protease inhibitor and enzyme inhibitor. For an average drug the probability is, if the bioactivity score is more than 0.00 then it is active, if -0.50 to 0.00 then moderately active and if less than -0.50 then inactive. On comparing the relative bioactivity scores of tacrine with synthesized compounds (**6–10**) for various classes, all the compounds displayed moderate to better results towards enzyme inhibition as evident from the Table 9, where compound **10** exhibited promising bioactivity score in comparison to other synthesized compounds. The standard drug tacrine showed highest bioactivity score 0.43 towards enzyme inhibition followed by compounds **10** > **7** > **8** = **6** > **9**. We have also compared the bioactivity score of the synthesized compounds (**6–10**) with the parent coumarin acid (**1**). The results obtained suggest that the parent coumarin acid (**1**) displayed lowest bioactivity score (-1.21) towards enzyme inhibition. It was concluded that the appending of propargyl group to the coumarin acids enhance their enzyme inhibition potency. The lowest bioactivity score and AChE inhibition of parent coumarin acid (**1**) was in good agreement with the docking study where parent coumarin acid (**1**) displayed unsatisfactory results. The bioactivity score data obtained for synthesized compounds was almost in collaboration with the AChE enzyme inhibition results where compound **10** showed promising AChE inhibition further validated by docking studies. The possible pharmacological effects and clarification of their potential as prodrugs will be an aim to another research.

3.6 Acetylcholinesterase Inhibition Docking Studies

Molinspiration calculations and prediction of molecular properties, values are within the limits, following Lipinski's rule, fulfilling the requirements of solubility, low

polar surface area and total hydrogen bond count are important predictors of good oral bioavailability. On the basis of lipophilicity, the synthesized compounds (**6–10**) are considered to be as oral drug/lead. The synthesized compounds were subjected to docking studies using Hex6.1, Discovery studio 4.0 Client and iGEMDOCK softwares to predict the binding mode of compounds towards target enzyme (PDB: 4ey4). The docking studies and their scoring functions gave crucial information regarding the orientation of the compounds and the strength of the non-covalent interaction (binding affinity) between molecules (ligand and receptor) in the binding pockets. On the basis of docking simulations, the strong binding affinity of compound **10** with AChE can be explained on the basis of hydrogen bonding as well as orientation and electronic features of the substituents towards the active site of the target enzyme Fig. 8f. The hydrogen bonds formed with amino acids of the protein showed good agreement with the predicted binding affinities obtained by molecular docking studies as verified by AChE inhibition activity data where compound **10** was found to be most potent AChE inhibitor ($IC_{50} = 0.21 \mu M$). The improved activity of the compound **10** in comparison to compounds **6**, **7**, **8** and **9** can be explained on the basis of its skeleton, that the presence of amine group at C-7 position of coumarin nucleus of compound **10**, enhances activity due to the formation of additional hydrogen bonds with amino acid residues PHE 531 and ALA 377 of the protein and easily perform as guest relation with receptor protein (host) Fig. 8f. In addition to this ester carbonyl in compound **10**, displayed hydrogen bonding interaction with the amino acid residue TRP 385. The docking studies revealed that the coumarin nucleus plays a major role in stabilizing the ligand–receptor complex by π -cation interactions with amino acid residue of the target protein as shown in Fig. 8. Moreover, anticholinesterase activity of the target compounds revealed that inhibition properties depend largely on the steric hindrance, orientation and electronic features of the substituents towards the active site and the combined effect of these features can determine the activity of the compounds. This steric effect can be seen operative in case of compound **9** with bulky $N(CH_3)_2$ substituent, rendering it less accessible to the active site of the target protein. Additionally, the π - π stacking interactions between the aromatic rings of coumarin nucleus with amino acid residues of the target enzyme further stabilizes the orientation of the molecule into the cavity of receptor as shown in Fig. 9. These extra interactions minimize the energy profile of the docked ligands and stabilize the position of ligands in the cavity of receptor (Fig. 10). Compound **6**, **7**, **8** and **9** displayed moderate profile of AChE inhibition. The AChE inhibition potency of compounds based on experimental biological

assay was seen in the order: Compound **10** > compound **7** > compound **8** > compound **6** > compound **9**. The empirical scoring function of iGemDOCK is the estimated sum total of vander waals and H-bonding energies. From the combined table and chart shown in Fig. 10, it is obvious that compound **10** demonstrated better affinity to receptor and showed maximum docking score as it was buried well inside the cavity of target protein.

4 Conclusions

The present work reports the facile, convenient and eco-friendly, silica-sulfuric acid assisted synthesis of bioactive ester derivatives of substituted coumarins. The present protocol offers attractive features such as excellent yields of the products in short times, mild reaction conditions, simple work-up procedure, environmentally benign, economic viability and reusability of the catalyst. We believe that this synthetic approach provides a better scope for the synthesis of ester derivatives of coumarin-3-carboxylic acids and will be a more practical alternative to the other existing methods. Moreover, information obtained from the results, suggest that these synthesized ester derivatives of coumarin-3-carboxylic acids can be used as templates for future research, for designing new entities through modification and derivatization with an improved AChE inhibition affinities for therapeutic purposes.

5 Supplementary information

Crystallographic data for structural analysis has been deposited with the Cambridge Crystallographic Data Centre, (CCDC) bearing no. 996160.

Acknowledgments Authors thank the Chairman, Department of Chemistry, A.M.U, Aligarh, for providing necessary research facilities, University Sophisticated Instrument Facility (USIF), AMU, Aligarh for providing SEM–EDX facilities, SAIF Panjab University Chandigarh for TEM analysis and spectral studies, Division of Bioscience, Dongguk University, Gyeongju, South Korea is acknowledged for bioassay and X-ray analysis. UGC is also gratefully acknowledged for research fellowship to Faheem Ahmad and Ali Mohammed Malla.

References

1. Ajani OO, Nwinyi OC (2010) J Heterocycl Chem 47:179
2. Weber US, Steffen B, Siegers CP (1998) Res Commun Mol Pathol Pharmacol 99:193
3. Patil AD, Freyer AJ, Drake SE, Haltiwanger RC, Bean MF, Taylor PB, Caranfa MJ, Breen AL, Bartus HR, Johnson RK, Hertzberg RP, Westley JW (1993) J Med Chem 36:4131

4. Yun BS, Lee IK, Ryoo IJ, Yoo ID (2001) *J Nat Prod* 64:1238
5. Cheng JF, Ishikawa A, Ono Y, Arrhenius T, Nadzan A (2003) *Bioorg Med Chem Lett* 13:3647
6. Zaha AA, Hazem A (2002) *Microbiologica* 25:213
7. Backhouse CN, Delporte CL, Negrete RE, Erazo S, Zuniga A, Pinto A, Cassels BK (2001) *J Ethnopharmacol* 78:27
8. Tada Y, Shikishima Y, Takaishi Y, Shibata H, Higuti T, Honda G, Ito M, Takeda Y, Kodzhimatov OK, Ashurmetov O, Ohmoto Y (2002) *Phytochemistry* 59:649
9. Stein AC, Alvarez S, Avancini C, Zacchino S, Poser GV (2006) *J Ethnopharmacol* 107:95
10. Whittaker M, Floyd CD, Brown P, Gearing AJH (1999) *Chem Rev* 99:2735
11. Maly DJ, Leonetti F, Backes BJ, Dauber DS, Harris JL, Craik CS, Ellman JA (2002) *J Org Chem* 67:910
12. Changwong N, Sabphon C, Ingkaninan K, Sawasdee P (2012) *Phytother Res* 26:392
13. Piazzi L, Cavalli A, Colizzi F, Belluti F, Bartolini M, Mancini F, Recanatini M, Andrisano V, Rampa A (2008) *Bioorg Med Chem Lett* 18:423
14. Garino C, Pietrancosta N, Laras Y, Moret V, Rolland A, Quéléver G, Kraus JL (2006) *Bioorg Med Chem Lett* 16:1995
15. Ortega DDS, Murphy BP, Velasquez FJG, Wilson KA, Xie F, Wang Q, Moss MA (2011) *Bioorg Med Chem* 19:2596
16. Radić Z, Reiner E, Simeon V (1984) *Biochem Pharmacol* 33:671
17. Radić Z, Reiner E, Taylor P (1991) *Mol Pharmacol* 39:98
18. Rudolf VS, Kovarik Z, Radić Z, Reiner E (1999) *Chem Biol Interact* 119–120:119
19. Pechmann VH, Duisberg C (1884) *Chem Ber* 17:929
20. Perkin WH, Henry WS (1875) *J Chem Soc* 28:10
21. Brufola G, Fringuelli F, Piermatti O, Pizzo F (1996) *Heterocycles* 43:1257
22. Cairns N, Harwood LM, Astles DP (1994) *J Chem Soc Perkin Trans* 1:3101
23. Shriner RL (1942) *The Reformatsky reaction*. Wiley, London, p 1:15
24. Yavari I, Shoar RH, Zonouzi A (1998) *Tetrahedron Lett* 39:2391
25. Al-Zaydi KM (2003) *Molecules* 8:541
26. Ghosh PP, Das AR (2012) *Tetrahedron Lett* 53:3140
27. Khoobi M, Ramazani A, Foroumadi AR, Hamadi H, Hojjati Z, Shafiee A (2011) *J Iran Chem Soc* 8:1036
28. Khurana JM, Kumar S (2009) *Tetrahedron Lett* 50:4125
29. Rao P, Konda S, Iqbal J, Oruganti S (2012) *Tetrahedron Lett* 53:5314
30. Khan AT, Das DK, Islam K, Das P (2012) *Tetrahedron Lett* 53:6418
31. Ray SK, Singh PK, Molleti N, Singh VK (2012) *J Org Chem* 77:8802
32. Bagdi AK, Majee A, Hajra A (2013) *Tetrahedron Lett* 54:3892
33. Salama TA, Ismail MA, Khalil AGM, Elmorsy SS (2012) *ARKIVOC* ix:242
34. Karami B, Khodabakhshi S, Eskandari K (2012) *Tetrahedron Lett* 53:1445
35. Jung JC, Lee JH, Oh S, Lee JG, Park OS (2004) *Bioorg Med Chem Lett* 14:5527
36. Zhang XS, Li ZW, Shi ZJ (2014) *Org Chem Front* 1:44
37. Karimian R, Piri F, Safari AA, Davarpanah SJ (2013) *J Nanostruct Chem* 3:52
38. Datta B, Pasha MA (2013) *ISRN Org Chem* 2013:1
39. Chavan F, Madje B, Bharad J, Ubale M, Ware M, Shingare M, Shinde N (2008) *Bull Catal Soc India* 7:41
40. Gawande MB, Hosseinpour R, Luque R (2013) *Curr Org Synth* 11:526
41. Heravi MM, Ajami D, Ghassemzadeh M (1999) *Synth Commun* 29:1013
42. Oskooie HA, Heravi MM, Sadnia A, Jannati F, Behbahani FK (2008) *Monatsh Chem* 139:27
43. Wu H, Shen Y, Fan LY, Wan Y, Zhang P, Chen CF, Wang WX (2007) *Tetrahedron* 63:2404
44. Shaterian HR, Ghashang M, Feyzi M (2008) *Appl Catal A Gen* 345:128
45. Baltork IM, Mirkhani V, Moghadam M, Tangestaninejad S, Zolfigol MA, Alibeik MA, Khosropour AR, Kargar H, Hojati SF (2008) *Catal Commun* 9:894
46. Zolfigol MA, Veisi H, Mohanazadeh F, Sedrpoushan A (2011) *J Heterocycl Chem* 48:977
47. Veisi H (2010) *Tetrahedron Lett* 51:2109
48. Shirini F, Zolfigol MA, Salehi P (2006) *Curr Org Chem* 10:2171
49. Zolfigol MA (2001) *Tetrahedron* 57:9509
50. Gawande MB, Branco PS, Varma RS (2013) *Chem Soc Rev* 42:3371
51. Gawande MB, Rathi AK, Nogueira ID, Varma RS, Branco PS (2013) *Green Chem* 15:1895
52. Bandgar BP, Gawande SS, Muley DB (2010) *Green Chem Lett Rev* 3:49
53. Breton GW (1997) *J Org Chem* 62:8952
54. Gupta R, Gupta M, Paul S, Gupta R (2009) *Bull Korean Chem Soc* 30:2419
55. Hasaninejad A, Zare AK, Sharghi H, Niknam K, Shekouhy M (2007) *ARKIVOC* xiv:39
56. Aoyama T, Suzuki T, Nagaoka T, Takido T, Kodomari M (2013) *Synth Commun* 43:553
57. Pramitha P, Bahulayan D (2012) *Bioorg Med Chem Lett* 22:2598
58. *International tables for X-ray crystallography*, vol III. Kynoch Press, Birmingham, England (1952)
59. SAINT, Version 6.02, Bruker AXS, Madison, WI (1999)
60. XPREP, Version 5.1, Siemens Industrial Automation Inc., Madison, WI (1995)
61. Sheldrick GM (1997) SHELXL-97: program for crystal structure refinement. University of Göttingen, Göttingen
62. Ellman GL, Courtney KD, Andres VJ, Feather-Stone RM (1961) *Biochem Pharmacol* 7:88
63. Ertl P, Rohde B, Selzer P (2000) *J Med Chem* 43:3714
64. Thomsen R, Christensen MH (2006) *J Med Chem* 11:3315
65. Schuttelkopf AW, Aalten DMFV (2004) *Acta Cryst D* 60:1355
66. Mustard D, Ritchie DW (2005) *Struct Funct Bioinform* 60:269
67. Discovery Studio v4.0 client Copyright ©2005-12 Accelrys software Inc
68. Hsu KC, Chen YF, Lin SR, Yang JM (2011) *BMC Bioinform* 12:1